Nuclear Instruments and Methods in Physics Research A318 (1992) 847–852
North-Holland

NUCLEAR
INSTRUMENTS
& METHODS
IN PHYSICS
RESEARCH
Section A

The "TEUFEL" undulator *

J.W.J. Verschuur, G.J. Ernst and W.J. Witteman
University of Twente, P.O. Box 217, 7500 AE Enschede, Netherlands

An overview of the design of the undulator for the Twente free electron laser is presented. The undulator is of the planar hybrid type, i.e. alternating permanent magnetic material and poles. The overall design is based on the method of Halbach. The flux balance is set up for the three-dimensional fluxes which are derived from the two-dimensional calculations. The undulator, using magnetic materials Sm_1Co_5 and 2V-permendur, has a wavelength of 25 mm. K value of 1, and a betatron wavelength (at equal focusing) of 300 mm for an electron beam of 6 MeV. An optimization is performed on a circular shape of the pole faces. The entrance and exit are tapered to allow a straight passage of the electron beam through the undulator. The tapering is adjusted to the requirements of minimal steering and displacement of the electron beam.

1. Introduction

The demands for the undulator for the Twente free electron laser are given by the operation conditions. A detailed description of the characteristics of the "TEUFEL" is presented in ref. [1]. The characteristics of FEL operation, important for the design of the undulator, are summarized below. Due to the high demands on the magnetic field in the undulator, the undulator is of the hybrid type, i.e. alternating permanent magnets and permeable poles. Several stages of optimization are performed on the dimensions of the undulator components. The desired FEL characteristics fix a few of the parameters. Of the remaining parameters some are set by optimization on the flux balance. The focusing properties of the undulator determine the shape of the pole. This optimization is done separately. The entrance and exit are designed separately using the results of the main design.

2. Design considerations and parameters

The parameters that set the design of the undulator can be grouped into two sets. First, we have the set of parameters that are fixed by the constraint of the desired operation of the FEL. The undulator parameter K has a favorable value of one, to obtain maximum gain at the fundamental wavelength. In the second stage of the project at an electron energy of 25 MeV the wavelength of the FEL light is chosen to be 10 μm. Therefore the wavelength of the undulator is fixed at 25 mm. The number of periods needed to reach saturation in a single pass at 6 MeV is about 50 [2]. The undulator parameter K and the wavelength λ_u of the undulator determine a desired amplitude of the first harmonic of the magnetic field of 0.61 T.

Parameters like gap, size of the magnets and size of the poles are set by optimization or can be chosen freely. The focusing properties of the undulator and the harmonic content of the magnetic field form additional constraints, that are used to fix the remaining parameters.

To reach the desired field strength with minimum material, a flux balance is set up to optimize the dimensions of the materials. The input for the flux balance comes from the two-dimensional flux calculations.

3. Flux balance

Given a design field amplitude of 0.61 T on the beam axis, we can set up a flux balance of the undulator. Due to the periodic structure and the high symmetry of the problem only a quarter period of the undulator has to be designed. In the other two directions only half of the structure (two other symmetry planes) has to be incorporated in the model. The method of design is based on that of Halbach [4]. Since no currents are present in the device and the fields are static, the analysis can be done on basis of scalar potentials. For the basic design the pole material is assumed to be infinitely permeable. This condition holds for fields well below the saturation level of the pole material

* Sponsored by "Nederlands Centrum voor Laser Research" (NCLR), the Dutch Foundation for Technological Research (STW) and the Dutch Foundation for Research on Matter (FOM).

2V-permendur. Only in a final check calculation the permeability is taken into account. The permanent magnetic material can be treated as charge sheet equivalent material (CSEM). This means that the relative permeability of the material is set to one and the magnetization is represented by (magnetic) charges. Having characterized the materials in this way, we can set up the flux balance in three-dimensional geometry. In the ideal case the magnetic field in the gap is completely determined by the potential and shape of the pole. The flux from the charges does not directly contribute to the field in the gap. The potential of the pole in turn is determined by the (magnetic) charges. This means that the flux, that is going from the charges to the poles, can be separated from the flux that is leaving the poles. Since no other fluxes are involved these two fluxes have to be equal. Fluxes from the charges are coming from the areas: interface, top, side and top corner. Fluxes that are leaving the pole are coming from the interface, bottom, top, side, top corner and bottom corner. For the flux coming from the CSEM and going in the pole we can symbolically write the following:

$$\Phi^{d} = \Phi_{i}^{d} + \Phi_{t}^{d} + \Phi_{s}^{d} + \Phi_{c}^{d}.$$

For the flux from the pole we write:

$$\Phi^{i} = \Phi_{i}^{i} + \Phi_{t}^{i} + \Phi_{b}^{i} + \Phi_{s}^{i} + \Phi_{c}^{i}.$$

The superscript indices d and i stand for direct and indirect, respectively and the subscript indices i, t, b, s, c stand for interface, top, bottom, side and corner, respectively.

To derive the various three-dimensional fluxes, the equivalent two-dimensional fluxes are calculated. This completes the flux balance for use in the design optimization.

The two-dimensional fluxes are calculated analytically, using the technique of conformal mapping and numerically using the POISSON group of codes [5]. These two-dimensional fluxes can best be described with the help of figs. 1a–c. Fig. 1a represents a three-dimensional view of a quarter period of the undulator. The coordinate frame is indicated in the figure. Fig. 1b is a slice of fig. 1a taken through the x–y-plane. Fig. 1c is a slice taken through the z–x-frame. The dimensions are indicated in the last two figures. Most of the two-dimensional fluxes can be calculated analytically (e.g. [4] and [6]). The flux balance then has the form of:

$$V_0 = h_2 H_{cB} \frac{\sum A^{d} x_i}{\sum A^{i} x_i},$$

where V_0 is the induced potential on the pole, h_2 is the height of the magnetic material and H_{cB} the coercive force of the magnetic material. The terms A, with superscripts i and d, are the dimensionless two-dimensional fluxes that are multiplied with the dimension in the third dimension denoted by x_i. The use of this equation in the design is describes below.

4. Design optimization

The optimization of the design is preceded by a few orientational calculations to get a rough predesign and to set the range of parameters. The optimization of the design itself is performed in three stages. First the influence of the overhang is related to the thickness of

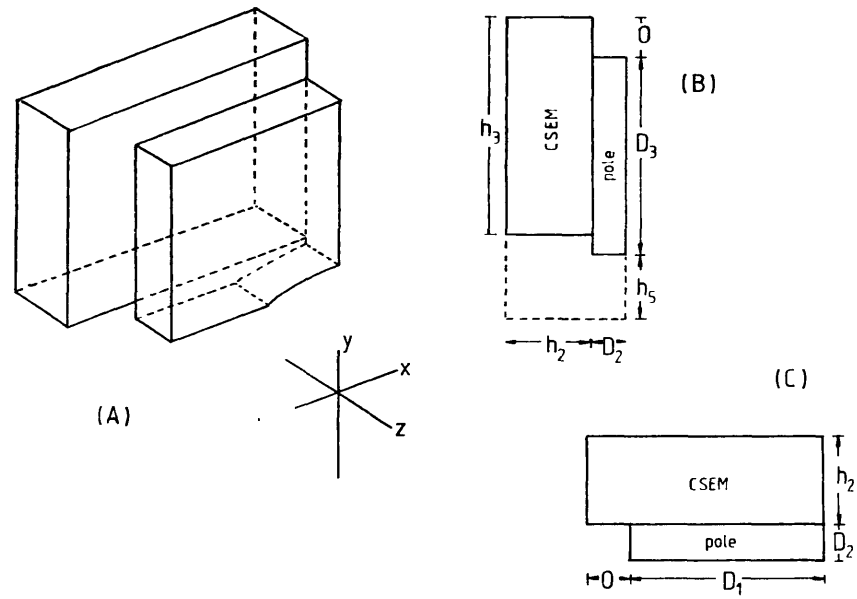

Fig. 1. Quarter period of the undulator and the corresponding two-dimensional cut-throughs in the $z-y$-plane and the $x-z$-plane.

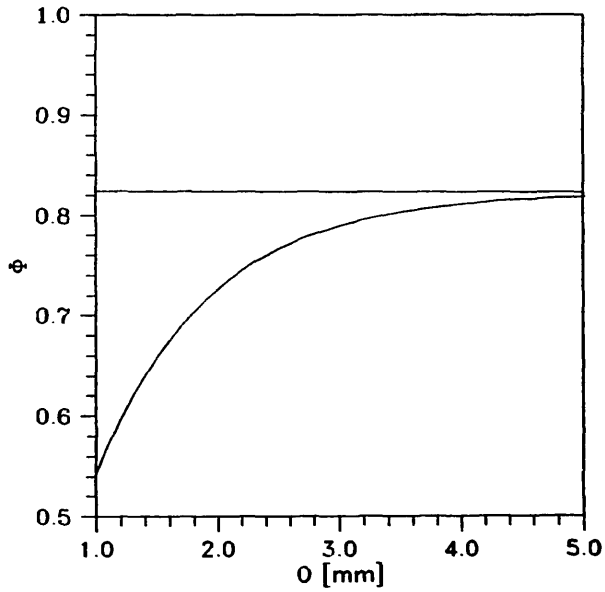

Fig. 2. Compensated flux loss due to overhang.

the magnetic material. In fig. 2 the compensation of the loss of flux from the pole is given as a function of the overhang. The overhang is normalized to the thickness of the magnetic material. To reduce the number of parameters in the optimization it was convenient to fix the overhang in this stage. The value chosen for the overhang is 1.4 times the half thickness of the magnetic material (h_2). With this value for the overhang about 78% of the flux, leaving the pole at the top and side, is compensated. This number is not completely independent of the thickness of the magnetic material, but in the range of $h_2 = 3.75$ to 4.74 mm for the half thickness of the pole the dependency can be neglected.

Second, the amplitude of the first harmonic of the magnetic field is calculated as a function of the thickness, the height of the pole and the gap distance. These calculations are performed numerically with the POISSON group of codes in two-dimensional geometry. The result for the amplitude of the first harmonic as a function of the thickness and the height of the pole is given in fig. 3. The dependence of the amplitude of the first harmonic on the gap distance is quite strong. Therefore the gap distance could be chosen independent of other parameters. For a gap of 8 mm the desired field strength could be reached. This value is used in the other calculations. From fig. 3, it is obvious that the thickness of the pole D_2 should be around 2.0 mm. The height of the pole should be no less than 40 mm. The harmonic content of the magnetic field consists of 4% in the third harmonic and less than 0.5% in the higher odd harmonics. In principle a complete suppression of the third harmonic is possible, but not desirable since it also leads to a reduction in the first harmonic.

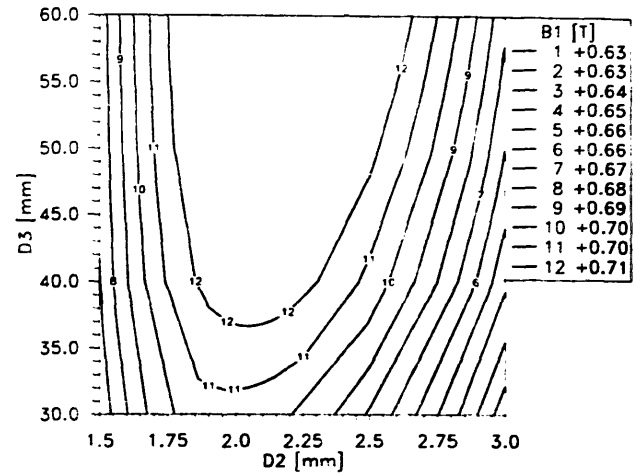

Fig. 3. First harmonic of the magnetic field B_1 as function of D_2 and D_3.

The third stage of the optimization is partially alternated with the second stage of optimization and concerns the complete flux balance in three-dimensional geometry. The most important parameters on which the flux balance depends are the height of the pole (D_3), the half thickness of the pole (D_2), the half width of the pole (D_1), the overhang of the magnetic material on the side (O), which is equal to the overhang on the top (O) and the half gap (h_5). The height of the magnetic material (h_3) is equal to $D_3 + O$ minus a small offset at the pole face. The flux balance can be written in the form.

$V_0 = \eta h_2 H_{cB}$.

From this we see that η (< 1) is a kind of performance parameter which has to be maximized varying the height D_3 and the half width D_1 of the pole. In fig. 4 η is plotted as a function of the half width of the pole D_1 and the height of the pole D_3. The dashed lines are lines of equal volume, important for the

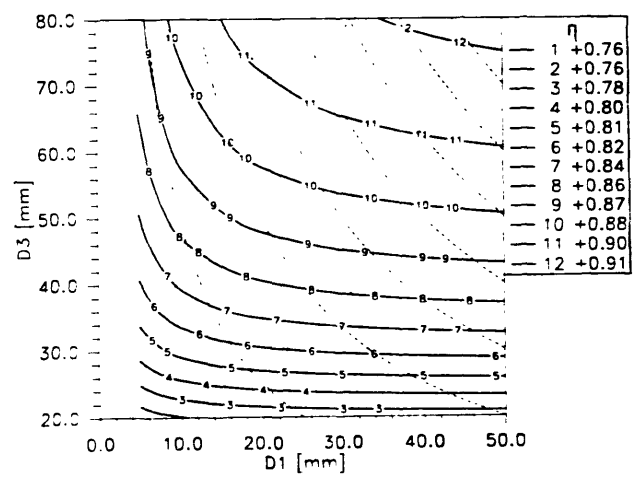

Fig. 4. Performance parameter η as function of D_1 and D_3.

Table 1

Design parameters		[mm]
Undulator wavelength	λ_u	25.0
Half gap	h_5	4.0
Overhang of magnet	O	6.0
Half thickness of pole	D_2	2.00
Half thickness of magnet	h_2	4.25
Height of pole	D_3	40.0
Height of magnet	h_3	45.0
Half width of pole	D_1	15.0
Half width of magnet	h_1	21.0

economical side of the design. An indication for the height of the pole D_3 from fig. 3 is 40.0 mm. From this number we see in fig. 4 that it is of no use to go beyond 15 mm for D_1. The main design is now set by the parameter values given in table 1.

5. Focusing

In the confinement of the electron beam through the undulator the betatron motion plays a significant role. The betatron motion is strongly dependent on the focusing. Although the focusing in the x-direction depends on the focusing in the y-direction, both focusing properties need not necessarily be equal in a planar undulator. However, it is useful to choose equal focusing in both directions. An analytical expression for the potential follows from the Poisson equation given the sinusoidal periodicity in the z-direction. The potential is given by:

$$\Psi = -\frac{b_0}{k_y}\cosh k_x x \sinh k_y y \sinh k_z z,$$

where k_x, k_y and k_z are the wave vectors in the x-, y-, and z-direction, respectively. To satisfy the Poisson equation one obtains the condition:

$$k_x^2 + k_y^2 = k_z^2,$$

where we choose for equal focusing, i.e.: $k_x = k_y = k_z/\sqrt{2}$. From the equations above one can see that the shape of an equal potential curve is a $\cosh(k_x x)$ in the x–y-plane. In an ideal planar undulator the focusing has to be of the sextupole type, which is done by the first two elements of the series expansion of the cosh function [7]. This can be met by removing a parabola segment out of the pole surface. Due to the error introduced by the finiteness of the pole surface an optimization around the ideal shape is needed. For practical reasons of construction we decided to optimize on a circle segment instead of a parabola segment. A verification of the focusing properties is performed in two-dimensional geometry. This method has its limitations, but the shape of the pole face near the electron beam stays close to the shape of an ideal equipotential surface. Calculated fields of the 2D configurations are shown in fig. 5. The focusing properties of the fields are compared. In fig. 5a we have focusing in the y-direction and a sinusoidal field in the z-direction. In fig. 5b we have defocusing in the y-direction and focusing in the x-direction. The defocusing in the

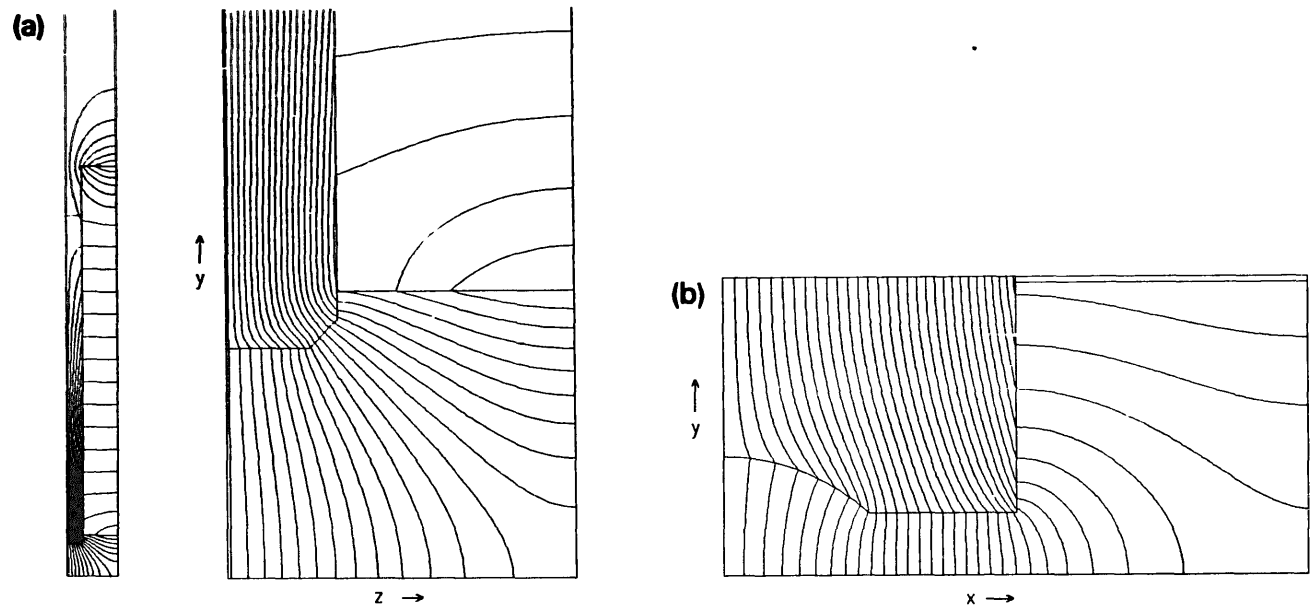

Fig. 5. (a) 2D field in the $y-z$-plane; (b) 2D field in the $x-y$-plane.

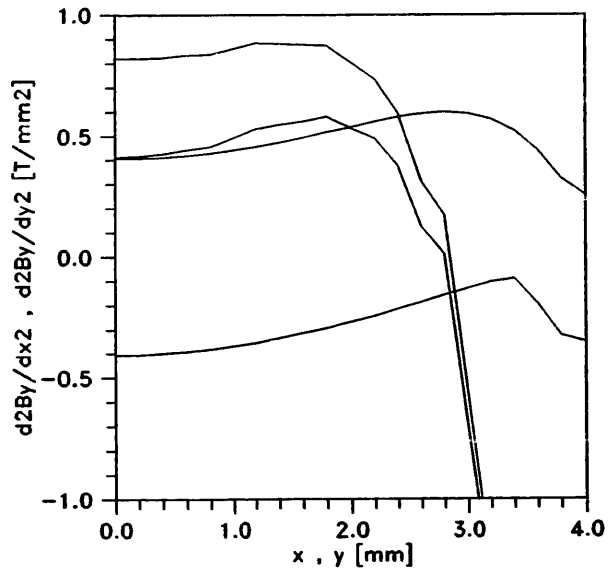

Fig. 6. Focusing properties of the fields shown in fig. 5.

y-direction in the x–y-plane is optimized to be half as strong as the focusing in the y-direction in the y–z-plane over a maximum beam area. We end up with an equal focusing in both x- and y-directions. This is illustrated in fig. 6, where the second derivatives of the fields of fig. 5 are shown. In this case the betatron wavelength is also equal for both directions. The betatron wavelength is given by:

$$\lambda_b = \beta\gamma\lambda_u/K,$$

where γ is the relativistic factor, $\beta = v/c$, K is the undulator parameter and λ_u is the undulator wavelength. In stage I of the "TEUFEL" project the energy of the electrons is 6 MeV leading to a γ of 12.7 and $\lambda_b = 0.45$ m, which results in about three periods over the length of the undulator. The betatron wavelength is also determined together with the electron beam emittance and the width of the electron beam in the undulator. The electron beam will be focused by a compact focusing system [8] at the entrance of the undulator to a diameter of 1.1 mm and the beam size will stay constant along the undulator. This value is well below the diameter of good focusing (4.8 mm), as can be seen from fig. 6.

6. Entrance and exit design

In order to avoid steering and displacement of the electron beam the entrance and exit of the undulator have to be tapered. The tapering will be performed by a successive reduction of the amount of magnetic material between the poles towards the beginning and end of the undulator. This will be done over two half periods. The poles at the entrance and exit will be equal to the poles in the undulator. This simplifies the design. Halbach [3] showed that a binomial excitation pattern of the poles is most desirable for tapered undulators. In order to reduce the steering it is suitable to have a second order binomial excitation pattern, i.e. an excited pole surrounded by two poles of half the excitation.

For calculation of the amount of magnetic material to reach the desired excitation pattern the undulator is represented by a C-network. The performance parameter η is related to the capacities. From the excitation pattern and the relation between the capacities the relation between the charges is then obtained. The charges represent the amount of magnetic material. From these calculations we found that the first magnet should have a volume of 0.1 times the volume of a magnet in the middle of the undulator and the second should have a volume that is 0.9 times the volume of a normal magnet. However the excitation of the beginning and end poles will be made adjustable by rotating magnets. A calculation was performed and the result is given in fig. 7. Details on the construction and the choice of the amount of rotatable magnetic material are still under study.

7. Status of the undulator

The magnetic part of the design of the "TEUFEL" undulator is almost complete. An important issue, still

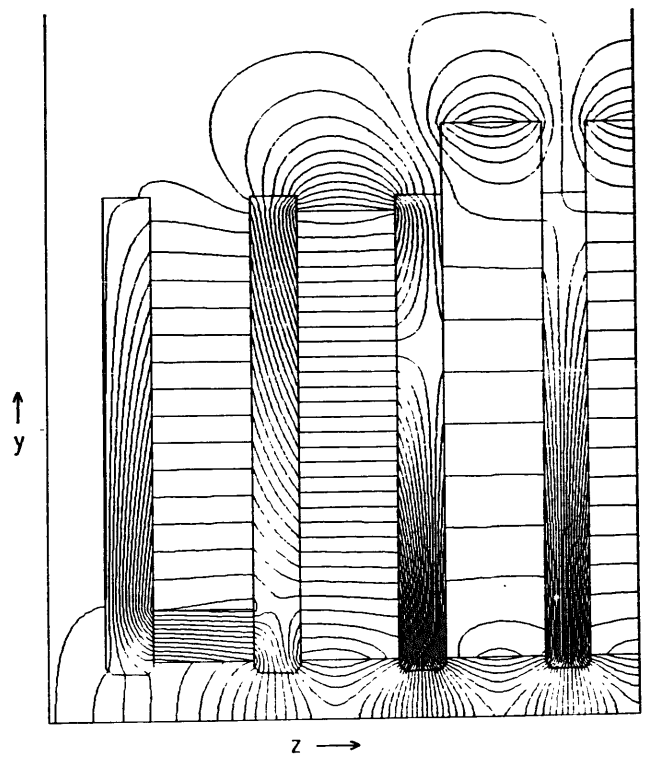

Fig. 7. Field calculation of the entrance and exit of the undulator.

under study, is the backing plane which shields the background magnetic fields. Also some minor parts of the entrance and exit design have to be finished. The magnetic material is at the stage of being ordered. The design of the mechanical construction is now being made.

References

[1] G.J. Ernst, W.J. Witteman, J.W.J. Verschuur, E.H. Haselhoff, R.F.X.A.M. Mols and A.F.M. Bouman, these Proceedings (13th Int. Free Electron Laser Conf., Santa Fe, USA, 1991) Nucl. Instr. and Meth. A318 (1992) 173.

[2] G.J. Ernst and J.C. Goldstein, these Proceedings (13th Int. Free Electron Laser Conf., Santa Fe, USA, 1991) Nucl. Instr. and Meth. A318 (1992) 649.

[3] K. Halbach, Nucl. Instr. and Meth. A250 (1986) 95.

[4] K. Halbach, Lectures at LBL, Berkeley, USA (1988); K. Halbach, Lectures at INEA, Milano, Italy, 1989, unpublished.

[5] POISSON-group of codes, LANL, Los Alamos, USA (1987).

[6] T. Meiander, SPIE 582 (1985) 193.

[7] E.T. Scharlemann, J. Appl. Phys. 58 (1985) 2154.

[8] R.F.X.A.M. Mols, G.J. Ernst and I.J.M. Botman, these Proceedings (13th Int. Free Electron Laser Conf., Santa Fe, USA, 1991) Nucl. Instr. and Meth. A318 (1992) 341.